Energy Efficient Depth Control for Underwater Devices Using Soft and Hard Actuators

Denizcan Koc[1], Wenyu Zuo[1], Fathi Ghorbel[2], Zheng Chen[3*]

Abstract— A Proton Exchange Membrane (PEM) fuel cell enabled buoyancy control device (BCD) is developed to address the challenge of depth control in underwater devices by compensating for buoyancy changes during underwater manipulations. The BCD splits distilled water into hydrogen and oxygen gases, increasing the volume of balloons attached to it, providing a permanent change in buoyancy of the device, and reducing the need for motors to run constantly. Results indicate that energy savings can reach up to 85% in comparison with experiments that use DC motors only. Additionally, the response is smoother and device stability is increased when DC motors are not running. Experimental results show the trajectory profiles when the BCD is active and passive, respectively. Furthermore, the PEM electrolyzers can be used as fuel cells to charge a battery or run another mechanical device after the operation, resulting in around 28% energy savings.

I. INTRODUCTION

Oil and gas industry uses a variety of underwater robotic technologies, including autonomous underwater vehicles (AUVs) and remotely operated underwater vehicles (ROVs) [1] for offshore oil and gas drilling and production. One of the biggest problems with underwater devices is the abrupt change in buoyancy [2], particularly with those that have to change overall weight as a result of capturing or releasing objects or materials in the water. One example in the industry is the study which investigates the effect of the Deepwater Horizon blowout on historic shipwreck-associated sediment microbiomes [3].

Attaching hard actuators to apply a thrust force, such as DC motors, against undesired movement of the device is the most frequent application for depth control [4]. One of the main reasons for it is that they can apply enough amount of power for actuation even when the weight is as much as tons [5]. Another reason is their ability to apply thrust in any desired direction if the motors are assembled in that direction accordingly. However, the usage of hard actuators to control the depth of the underwater device has also significant shortcomings in terms of huge energy usage and large noise and turbulence creation [6]. When there is

a change in the total mass of the device, it is not neutrally buoyant anymore, so it will need thrust force continuously generated while it is in operation. Running the DC motors all the time in operation would require too much energy consumption. This situation is the main motivation behind the study to find an alternative method for underwater depth control.

A basic solution to prevent DC motors to run for all the time is nothing but adjusting the mass or volume of the device in such way that it can change its buoyancy and becomes stable. In the past, several studies have been done in the Bio-inspired Robotics Control Lab at the University of Houston to bring that solution. One example was using the PEM fuel cells only (without DC motors) by using PID control [7]. The reasons behind using water electrolysis instead of common methods such as using pumps and compressed air are to prevent the noise and energy consumption of pumps and prevent the shortcoming of having a limited amount of air [8]. There are other examples including improved control methods for the same system by using auto-tunned PID control [9] [10], optimal trajectory planning control [11], Proportional-Integral-Derivative-Acceleration (PIDA) control [8] and Proportional-Derivative-Acceleration (PDA) control [12] [13]. The main motivation behind the idea of using DC motors and PEM fuel cells in combination is the slow response of PEM fuel cells underwater. DC motors can apply the necessary force to track the desired depth until fuel cells are able to bring the device to a neutrally buoyant level.

There are no previously presented experimental results of buoyancy control using DC motors and PEM fuel cells in combination, which brings a clear novelty to our study. This study includes experimental results with high efficiency and an examination of the energy that can be used as a benefit after the operation. Additionally, it estimates the efficiency for real-time applications under higher pressures and weights and conducts a feasibility study for possible real-time applications using much heavier devices at much higher pressures.

II. MODELING OF THE ROBOT

A. State Space Model

The schematic and free-body diagram of the device can be observed in Figure 1. The propellers should be located in a way that they apply thrust force in the vertical direction only, and they do not lead to any other movements such as rotation. Therefore, it is decided to use two propellers which are turning in opposite directions, and they are assembled to the right and left-hand sides of the device. The BCD has

balloons above it because it is needed to keep the balloons away from the running part of the DC motors in order to prevent any damage. The device has one constant and one variable volume, those are V_1 and V_2, respectively. The V_1 basically represents every volume rather than the volume of balloons, and V_2 represents the volume of balloons. The depth of the device is represented as "x", which is increasing from the bottom to the surface. The only force which is in the opposite direction is the weight of the device, which is represented as W. The forces in the positive direction of x are the drag force, which is represented by $F_d(t)$, the buoyancy force, which is represented by $F_b(t)$, and the thrust force, which is represented by F_t. Drag force is the aerodynamic force that is caused by the contact and interaction between the device and the fluid. It is directly proportional to the velocity of the device. The buoyancy force is related to the instantaneous volume of the device, which can be also counted as related to the displacement because the variable volume of the balloons is controlled based on the depth data coming from sensors. The thrust force is related to the feedback from the depth only. The mathematical expression which summarizes the equation of motion can be written as follows:

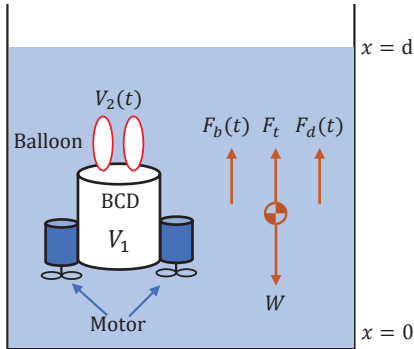$$F_{net} = -W + F_b(t) + F_t + F_d(t), \qquad (1)$$

Fig. 1.   Schematic of the device

The terms in the equation of motion can be expressed individually as follows:

$$F_b(t) = \rho(V_1 + V_2(t))g, \qquad (2)$$

$$F_d(t) = b\dot{x}^2(t), \qquad (3)$$

$$W = mg, \qquad (4)$$

$$F_t = \tau, \qquad (5)$$

where the fluid's density of the water represented as ρ, gravitational acceleration is represented as g, drag coefficient is represented as b, total mass of the device represented as m, and the thrust force is represented as τ. This parameter can be considered as the control input of the system because it will be directly related to the voltage input to the system.

By considering equations from Eq. 1 to Eq. 5, the state space representation of the system can be expressed as follows:

$$\begin{bmatrix} \dot{X}_1 \\ \dot{X}_2 \end{bmatrix} = \begin{bmatrix} X_2 \\ \frac{b}{m}X_2^2 + \frac{\rho g}{m}V_1 - g \end{bmatrix} + \begin{bmatrix} 0 & 0 \\ 1 & \frac{\rho g}{m} \end{bmatrix} \begin{bmatrix} \tau \\ V_2 \end{bmatrix} \qquad (6)$$

The task is to design an appropriate controller which should adjust the hard actuator (τ) and the soft actuator (V_2) in a way that gives a smooth tracking of reference depth.

B. Parameter Identification

1) Parameters Identification for the PEM Fuel Cells: When the device is neutrally buoyant, the weight of the device is measured. The volume of the device is calculated from this information because only nonzero terms are buoyancy force and weight in Newton's Second Law, which can easily give the total volume. It is found as $1.204 \cdot 10^{-3} \ m^3$. This number represents the total volume of the device when there is no gas in the balloons, assuming the volume of extra weights to make the device slightly negative buoyant is negligible.

Another experiment has been monitored to figure out what would be the increasing velocity of V_2, which is the variable volume of balloons. Firstly, the weight is increased slightly so that it becomes slightly negatively buoyant, and BCD is activated and waited for the device to come to a neutrally buoyant level. By solving the equations of motion in these two different cases, the first and second volumes are figured out. Thus, the difference gives the volume of balloons (V_2). In order to find the increasing velocity of V_2, it has basically been divided by the time that passed. It includes an assumption for sure that the rate is constant, however, it should be accurate enough to simulate the dynamics of the device effectively to design the controller. According to the result, the increasing rate of the volume due to the fuel cells ($\dot{V}_2$) is $1.364 \cdot 10^{-7} \frac{m^3}{s}$.

2) Parameter Identification of the Propellers: Experiments have been done on DC motors to find the linear mapping of the relation between the voltage applied to DC motors and thrust force in order to simplify the model. It is observed that $77.4 \ g$ weight can be lifted by one single propeller if the applied voltage is set to 2.5 V. Because of the very tiny volume of weights and very small buoyancy force of the propellers (compared to weight), it is assumed that only carrying force is the thrust force of propellers in order to use the equation of motion to find thrust force. Thus, the thrust force, in that case, is as follows:

$$F_t = 0.0774 kg \cdot 9.81 \frac{m}{s^2} = 0.76 \text{ N}.$$

Mechanical devices likely have a dead-zone in a small range of voltage [14]. The major cause for the dead-zone is the Coulomb friction force [15]. From the experiments, one can clearly observe that DC motors also have a dead-zone between 0V - 5V. For the sake of having a mathematical representation for the model, it is assumed that there is a linear proportional relationship between the applied voltage and the thrust force, which starts after 0.5V. If the applied

voltage is represented as V_{app}, the thrust force in terms of applied voltage can be expressed as follows:

$$F_t = \frac{(V_{app} - 0.5V)}{2} \cdot 0.76 \text{ N} \cdot 2 = (V_{app} - 0.5V) \times 0.76 \text{ N} \quad (7)$$

The reason for multiplication with 2 is there are two propellers connected to the device. The second term on the right-hand side of the Eq. 6 includes two control parameters, which are V_2 and τ. Those can be used as control parameters of the device. The detailed design for adjusting them will be explained in Section III.

III. CONTROL SYSTEM DESIGN

The control system of the device includes two control inputs and one output. The control inputs are the voltage input to the DC motors and the voltage input to the BCD for water electrolysis. The output is the depth of the device, which feds the inputs automatically with the closed-loop control system as shown in Figure 2. An onboard pressure sensor is used to take the depth data. The difference between instantaneous depth and reference depth is giving the error signal in the controller. It both feds the propellers which are providing thrust force, and fuel cells which are able to generate hydrogen and oxygen gases to the inside of balloons, so that the balloons can be able to increase the buoyancy force. A detailed discussion about the control systems for propellers and fuel cells can be found in the following subsections.
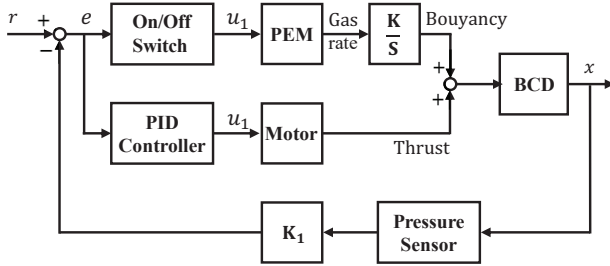

Fig. 2. Control system diagram.

A. Control of Propellers

PID control is used to control the speed of propellers by adjusting the voltage supplied to the DC motors. The control loop takes in the current depth of the device, which is measured using a pressure sensor and compares it to the target depth. The difference between these two values is the error that goes to the controller. The output of the control loop is a voltage input to the motors, which is directly proportional to their speed and the resulting thrust force. The overall process can be described mathematically as follows:

$$\tau(t) = K_p e(t) + K_d \dot{e}(t) + K_i \int e(t)\,dt \quad (8)$$

The parameters K_p, K_d, and K_i are determined by using the auto-tuning feature of MATLAB Simulink based on the simulated model.

B. Control of BCD

Changes in the voltage supplied to PEM fuel cells cannot produce sudden movements because the gas generation rate is low and it takes time for the depth of the device to change. This is why propellers are needed at the start to keep the device at the desired level without waiting too long. The control system for fuel cells should operate at maximum power when the difference between the current and desired depths is significant, in other words, it should use maximum power until the device becomes neutrally buoyant. Therefore, the controller for BCD is designed to work with maximum capacity to do water electrolysis when it is needed to make the device more buoyant and to work with maximum capacity in the reverse process when the device needs to be less buoyant.

The error boundary is 5 mm (the error is assumed as significant above that point and insignificant under that point). "e" is the error, and V_{input} is the voltage input to the fuel cells. The controller equations are expressed in Table I, where V_{max} represents the voltage that can run the fuel cells

TABLE I
CONTROL INPUT OF THE PEM FUEL CELLS

Conditions	$e > 5$ mm	$e < 5$ mm
$e > 0$	V_{max}	0
$e < 0$	$V_{max,inv}$	0

with maximum power, and $V_{max,inv}$ represents the maximum capacity to run in the reverse mode.

The main purpose of the simulation was to find the optimal values for the PID controller of the propellers using the auto-tuning feature. The results of the auto-tuning were used to determine the optimal values for the controller, which will be used to optimize the control of the propellers.

The results of the auto-tuning feature in MATLAB Simulink were used to determine the optimized values for the PID controller of the propellers, which are 0.647, 0.0312, 3.199, and 2.123 for the "P", "I", "D" gains and filter coefficient ("N"), respectively. These values were used for further real-time experiments, and the simulated response profile is shown in Figure 3.
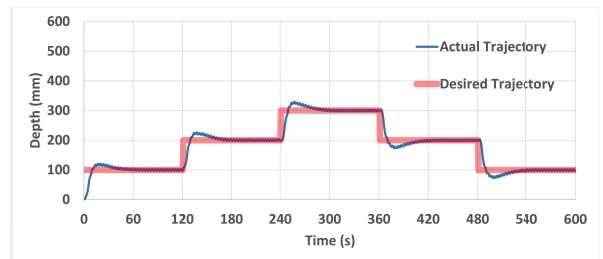

Fig. 3. Response profile of the simulation.

IV. Experimental Validation

A. Design and Experimental Setup of the Device

An underwater device, which has depth control by hard and soft actuators is developed. The basic structure of the device can be observed in Figure 4. The integrated parts to the structure are a buoyancy control device (BCD) that handles the water electrolysis [13], water-proof propellers that are used for thrust force, and one water-proof gripper which makes the device able to grab, move and release items.
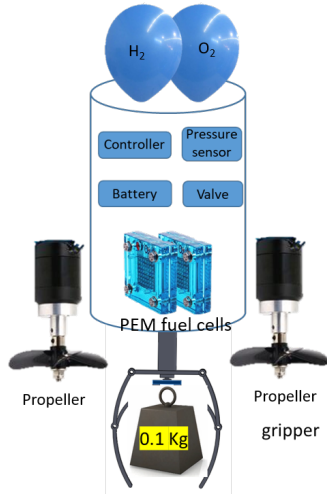

Fig. 4. Design of the service robot using both soft and hard actuators.

As it can be observed from Figure 5, the device is composed of two DC motors (LICHIFIT, ASIN:B07WY4MDYZ), two PEM fuel cells (Horizon, SKU: HFC-FCSU-023B) with two balloons and one water tank connected to them, one pressure sensor (SparkFun, MS5803-14BA), one gripper, buoyancy foams, and some extra weights. The pressure sensor is used to measure the depth underwater. Foams are used as positive buoyant material, and extra weights are used as negative buoyant material to keep the device vertical. They have adjusted in a way that the device becomes slightly negatively buoyant. The electrolyzers are connected to each other and the water tank in a way that the oxygen output of the first electrolyzer is going to the water tank. It is separated from its liquid part in a water tank, and pure oxygen gas (without liquid) is coming to the second electrolyzer. For that reason, the second electrolyzer can provide dryer gas to the balloons. This is the main reason to use two electrolyzers in series instead of one.

The detailed structure of the buoyancy control device can be seen in Figure 5. The electrolyzers are capable of working in two modes. The first mode is water electrolysis mode. In this mode, they are used as water electrolysis devices. They can convert the water to hydrogen and oxygen gases by taking an electrical input. By using them in this mode, the volume of the balloons can get larger, therefore, the buoyancy force of the device can get larger. On the other hand, when they are in fuel cell mode, they can use the oxygen and hydrogen gases and produce water and electricity

from them [16]. As a result of this process, the volume of the balloons is getting decreases, which leads the buoyancy force of the device to get decreased. Furthermore, there is a smaller amount of energy output when the device is working in this mode (compared to the energy input in the other mode). This energy can be used to charge a battery by a boost converter between them (because of a small amount of voltage), or to run another electrical system. In the experiment of this study, the system is connected to an external propeller device, and the device is made to be able to give energy to this external propeller when electrolyzers are in fuel cell mode by using a relay module.
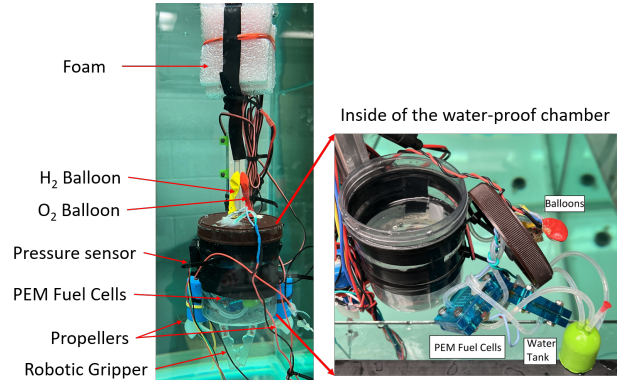

Fig. 5. Prototype of the service robot.

B. Experimental Results

In order to make a conclusion about the effect of BCD when it is added to the device as a controller, two separate experiments have been done with and without BCD. The first one includes the usage of DC motors without any help from BCD. The target depth was set to 50 mm from the bottom for the first 120 seconds, 100 mm from the bottom for the next 120 seconds, and 150 mm from the bottom for the final 120 seconds. After that point, the desired depth was reduced symmetrically to this process. Figure 6 shows the recorded data from the depth sensor. As can be observed, after a transient period, the device settles near the desired depth with small oscillations and the transient period is short when the desired depth is changed.
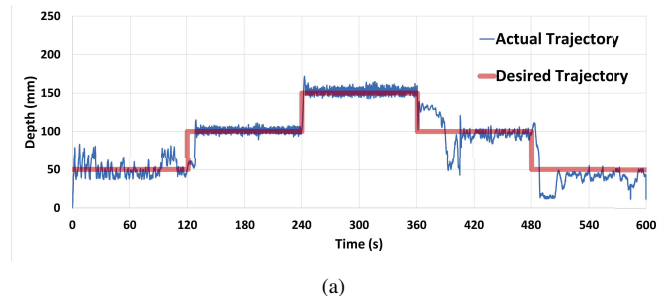

(a)

Fig. 6. Step tracking results with propellers working only.

Another experiment has been done by running both propellers and BCD. In order to make a more accurate observation, the target depth profile has been kept the same within the same time periods. Figure 7 includes the recorded data from the depth sensor, including noise cancellation. As can be observed from the figure, except for some time periods which include small oscillations, the profile becomes much more accurate and smooth. The main reason is that the BCD is able to bring the device to a neutrally buoyant level at around that time, so there is no movement to the bottom due to the weight of the device after that time. Therefore, DC motors do not have to run anymore. It is totally balanced with extra buoyancy provided by the PEM fuel cells.
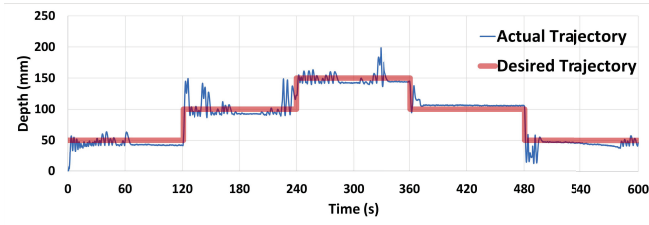
(a)

Fig. 7. Step tracking results with both propellers and fuel cells working.

C. Effect of Fuel Cells on the Energy Consumption

The DC motors and BCD are powered with a single power generator, which provides 9.1 V voltage. The H-bridge is used to adjust the input signals to the DC motors and BCD by taking the online data from Arduino. By multiplying the current data with the constant voltage that the power generator applies, and integrating it with respect to the time, the total consumed energy for the case without fuel cells is founded as 3965 J, and the total consumed energy for the case with fuel cells is founded as 594 J. According to the current recordings of BCD, 45 J out of 594 J is spent for BCD, and the rest is spent for running the DC motors. Therefore, the total energy saving when fuel cells are used is:

$$E_{saving} = 3965 \text{ J} - 594 \text{J} = 3371 \text{ J},$$

which can be expressed with percentages as follows:

$$E_{saving} = \frac{3371 \text{ J}}{3965 \text{ J}} \cdot 100 = \textbf{85\%}.$$

Therefore, if the BCD is used in addition to DC motors in the experiment, the percentage of energy saving can be 85%, which is a significant change even though the time period of the experiment is as small as 600 seconds.

After the experiment, the PEM electrolyzers are connected to a propeller that needs a small amount of current to run. The purpose was to observe how much energy can be taken back from electrolyzers. It has been observed that they are able to run the propeller for 260 s.

Considering that the average voltage of the electrolyzers is observed as 0.5 V in reversible mode, the total energy that has been taken back from the electrolyzers is founded

as 12.4 J. Therefore, the efficiency of PEM electrolyzers can be represented in percentages as follows:

$$\varepsilon = \frac{12.4 \text{ J}}{45 \text{ J}} \cdot 100 = \textbf{28\%}$$

It should be noted that the efficiency of PEM electrolysis is expected around 75% [17], and the efficiency of PEM fuel cell is expected around 40% [18]. Therefore, by multiplying those, an efficiency of around 30% is expected. The experimental result is close enough to validate this estimation.

V. ESTIMATIONS ON REAL-TIME APPLICATIONS OF HEAVY DEVICES IN DEEP OCEAN

Although experiments show that BCD is helping to reduce energy consumption significantly, it might be a concern whether it will be applicable for much heavier devices under high pressures in the deep ocean. The calculations based on basic information about PEM water electrolysis and gas behaviors will be provided in this chapter and will be analyzed to see whether the results are realistic for real-time applications or not.

If it is assumed that it is desired to grab an item that has 5 kg weight with ignorable volume, the necessary extra volume to make the device neutrally buoyant after the application would be 0.0048 m^3. It will be tried to find whether the produced hydrogen and oxygen can occupy this amount of volume under the conditions that are defined.

The density of the hydrogen is 20 kg/m^3 at 300 bars [19], which corresponds to around 3000 meters. By using the density information of hydrogen, it can be found that the necessary amount of hydrogen will be 0.096 kg to occupy the amount of volume of 0.0048 m^3.

The next consideration should be whether this application will be energy efficient or not. The necessary thrust force to balance 5 kg extra weight can be estimated from the experimental results. In the experiment, the extra weight which makes the device negative buoyant was around 20 g. The energy consumption rate can be assumed 250 times larger because the extra weight is 5 kg instead of being 20 g. If it is assumed that the device will work for 1 hour underwater, the consumption will be 6 times larger because the experiment took 10 minutes instead of 1 hour. The total cost of energy can be roughly founded as 5947.5 kJ.

In order to estimate the energy saving, how much energy will it take to use BCD should also be founded in addition to DC motors. The PEM water electrolysis needs around 67 kW power to produce one kg of hydrogen [20]. The amount that is needed corresponds to approximately 6.5 kW while the production rate is 10 kgh^{-1}. The hydrogen production rate depends on many factors such as the size of the electrolyzer, the type of electrodes used, the type of PEM used, and the concentration of the electrolyte solution. In the calculations, it will be assumed as 1 kgh^{-1} in order to be more reliable. The energy consumption rate can be estimated as 0.65 kW since the hydrogen production rate is 10 times less compared to 10 kgh^{-1}. For the amount of hydrogen that is needed, around 6 minutes should be spent. Although it might seem

low, it is known that the efficiency of PEM water electrolysis is higher when pressure is increased [21].

By using the estimation for the energy consumption rate of BCD, it can be concluded that the BCD would spend 234 KJ to run for 6 minutes. Moreover, running the DC motors for 360 seconds would lead us to spend 594.8 KJ. Summing this with the result for BCD, the estimation for total energy consumption becomes 828.8 KJ. As a result, the percentage of energy saving can be calculated as follows:

$$E_{saving} = \frac{5947.5\ kJ - 828.8\ kJ}{5947.5\ kJ} \cdot 100 = \mathbf{86\%}$$

If the calculation for different amounts of time of operations is repeated, the relation can be seen in Figure 8.
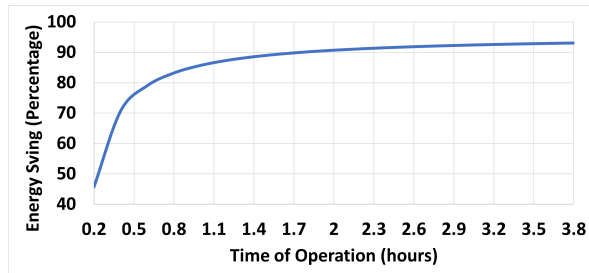

Fig. 8.   The energy saving with respect to the time of operation.

VI. Conclusion and Future Work

This paper presents an energy-efficient depth control that incorporates both hard and soft actuators. The design aims to address the problems of excessive energy consumption with hard actuators alone and slow response speed with soft actuators alone. The control methods used are PID control for hard actuators and switching on-off control for soft actuators. The parameters were selected based on simulations. The experimental results show that the chosen parameters are effective in providing a fast and smooth response. A comparison was made between a system using only hard actuators and a system using both hard and soft actuators, demonstrating that the combined system consumes less energy and provides a more accurate and smooth response. The ROVs and AUVs are generally much heavier than what is tried and work under high pressure. Estimation for a larger weight and higher pressure scenario is presented based on the available knowledge on fuel cells up to now. Future work should be continued by doing experiments with heavier devices under much higher pressures.

VII. ACKNOWLEDGMENT

REFERENCES

[1] L. L. Whitcomb, "Underwater robotics: Out of the research laboratory and into the field," in *Proceedings 2000 ICRA. Millennium Conference. IEEE International Conference on Robotics and Automation. Symposia Proceedings (Cat. No. 00CH37065)*, vol. 1.   IEEE, 2000, pp. 709–716.

[2] T. I. Um, Z. Chen, and H. Bart-Smith, "A novel electroactive polymer buoyancy control device for bio-inspired underwater vehicles," in *2011 IEEE International Conference on Robotics and Automation*.   IEEE, 2011, pp. 172–177.

[3] L. J. Hamdan, J. L. Salerno, A. Reed, S. B. Joye, and M. Damour, "The impact of the deepwater horizon blowout on historic shipwreck-associated sediment microbiomes in the northern gulf of mexico," *Scientific reports*, vol. 8, no. 1, pp. 1–14, 2018.

[4] B. K. Tiwari and R. Sharma, "Design and analysis of a variable buoyancy system for efficient hovering control of underwater vehicles with state feedback controller," *Journal of Marine Science and Engineering*, vol. 8, no. 4, p. 263, 2020.

[5] C. Yue, S. Guo, M. Li, and L. Shi, "Electrical system design of a spherical underwater robot (sur-ii)," in *2013 IEEE International Conference on Information and Automation (ICIA)*.   IEEE, 2013, pp. 1212–1217.

[6] H. Kang, "The study of dc motor noise and vibration," *SAE transactions*, pp. 2461–2467, 1995.

[7] J. Yazji, A. L. J. Keow, H. Zaidi, L. T. Torres, C. Leroy, and Z. Chen, "Buoyancy control device enabled by reversible proton exchange membrane fuel cells for fine depth control," *Journal of Dynamic Systems, Measurement, and Control*, vol. 143, no. 3, 2021.

[8] A. Keow, Z. Chen, and H. Bart-Smith, "Pida control of buoyancy device enabled by water electrolysis," *IEEE/ASME Transactions on Mechatronics*, vol. 25, no. 3, pp. 1202–1210, 2020.

[9] A. Keow and Z. Chen, "Auto-tuning control of pem water electrolyzer," in *Dynamic Systems and Control Conference*, vol. 59155.   American Society of Mechanical Engineers, 2019, p. V002T22A005.

[10] A. L. J. Keow and Z. Chen, "Auto-tuning control of proton exchange membrane water electrolyzer with self-assessment and gain scheduling," *Journal of Dynamic Systems, Measurement, and Control*, vol. 143, no. 5, 2021.

[11] W. Zuo, X. Yi, F. H. Ghorbel, and Z. Chen, "Optimal trajectory planning and control of buoyancy control device enabled by water electrolyzer," in *2019 IEEE 58th Conference on Decision and Control (CDC)*.   IEEE, 2019, pp. 2120–2125.

[12] A. Keow, W. Zuo, F. Ghorbel, and Z. Chen, "Underwater buoyancy and depth control using reversible pem fuel cells," in *2020 IEEE/ASME International Conference on Advanced Intelligent Mechatronics (AIM)*.   IEEE, 2020, pp. 54–59.

[13] A. L. J. Keow, W. Zuo, F. Ghorbel, and Z. Chen, "Reversible fuel cell enabled underwater buoyancy control," *Mechatronics*, vol. 86, p. 102865, 2022.

[14] J. O. Jang, "A deadzone compensator of a dc motor system using fuzzy logic control," *IEEE Transactions on Systems, Man, and Cybernetics, Part C (Applications and Reviews)*, vol. 31, no. 1, pp. 42–48, 2001.

[15] T. Kara and I. Eker, "Nonlinear modeling and identification of a dc motor for bidirectional operation with real time experiments," *Energy Conversion and Management*, vol. 45, no. 7-8, pp. 1087–1106, 2004.

[16] D. Falcão and A. Pinto, "A review on pem electrolyzer modelling: Guidelines for beginners," *Journal of Cleaner Production*, vol. 261, p. 121184, 2020.

[17] M. Carmo, D. L. Fritz, J. Mergel, and D. Stolten, "A comprehensive review on pem water electrolysis," *International journal of hydrogen energy*, vol. 38, no. 12, pp. 4901–4934, 2013.

[18] F. Barbir and T. Gomez, "Efficiency and economics of proton exchange membrane (pem) fuel cells," *international journal of hydrogen energy*, vol. 22, no. 10-11, pp. 1027–1037, 1997.

[19] S. Makridis, "Hydrogen storage and compression," *arXiv preprint arXiv:1702.06015*, 2017.

[20] R. Hancke, T. Holm, and Ø. Ulleberg, "The case for high-pressure pem water electrolysis," *Energy Conversion and Management*, vol. 261, p. 115642, 2022.

[21] H. Michishita, H. Matsumoto, and T. Ishihara, "Effects of pressure on the performance of water electrolysis of the cell using nafion membrane electrode," *Electrochemistry*, vol. 76, no. 4, pp. 288–292, 2008.